Sevoflurane suppresses cell viability and invasion and promotes cell apoptosis in colon cancer by modulating exosome-mediated circ-HMGCS1 via the miR-34a-5p/SGPP1 axis

JUAN HE, HUAPING ZHAO, XING LIU, DONGMEI WANG, YONG WANG, YANQIU AI and JIANJUN YANG

Department of Anesthesiology and Perioperative Medicine, The First Affiliated Hospital of Zhengzhou University, Zhengzhou, Henan 450000, P.R. China

Received December 11, 2019; Accepted July 16, 2020

DOI: 10.3892/or.2020.7783

Abstract. As a novel halogenated hydroxyl ether-inhaled general anesthetic, sevoflurane has been reported to affect the progression of diverse human cancers. In the present study, we aimed to explore the functions and underlying mechanisms of sevoflurane in colon cancer. MTT assay, flow cytometric analysis and Transwell assay were conducted to evaluate cell viability, apoptosis and invasion, respectively. Western blot analysis was performed to determine the protein level of sphingosine-1-phosphate phosphatase 1 (SGPP1). The morphology and size of exosomes were analyzed by TEM and NTA. The levels of circular RNA 3-hydroxy-3-methylglutaryl-CoA synthase 1 (circ-HMGCS1), microRNA (miR)-34a-5p and SGPP1 mRNA were examined by RT-qPCR. Dual-luciferase reporter and RNA RIP assays were utilized to explore the interaction between miR-34a-5p and circ-HMGCS1 or SGPP1. A murine xenograft model was established to investigate the effect of circ-HMGCS1 *in vivo*. As a result, it was determined that sevoflurane suppressed cell viability and invasion and induced apoptosis in colon cancer in a dose-dependent way. Exosomal circ-HMGCS1 was increased in the serums and cells of colon cancer patients. Circ-HMGCS1 was downregulated by sevoflurane treatment in colon cancer cells and circ-HMGCS1 overexpression could restore the effect of sevoflurane on colon cancer cell development. miR-34a-5p was a target of circ-HMGCS1 and miR-34a-5p inhibition reversed the effect of circ-HMGCS1 silencing on colon cancer cell progression. Moreover, circ-HMGCS1 knockdown suppressed SGPP1 expression via sponging miR-34a-5p. Knockdown of circ-HMGCS1 blocked tumor growth *in vivo*. In conclusion, sevoflurane inhibited colon cancer progression by modulating the exosome-transmitted circ-HMGCS1/miR-34a-5p/SGPP1 axis.

Correspondence to: Dr Jianjun Yang, Department of Anesthesiology and Perioperative Medicine, The First Affiliated Hospital of Zhengzhou University, 1 Jianshe East Road, Zhengzhou, Henan 450000, P.R. China
E-mail: fcchej2@zzu.edu.com

Key words: colon cancer, sevoflurane, exosome, circ-HMGCS1, miR-34a-5p, SGPP1

Introduction

Colon cancer is a lethal malignancy in the gastrointestinal tract with high incidence and recurrence, leading to approximately 1,096,601 new cases and 551,269 deaths in 2018 (1-3). Currently, the methods of colon cancer therapy are surgery combined with chemotherapy, radiotherapy and targeted therapy (4). Although treatment methods have advanced, the incidence of colon cancer continues to increase and the prognosis of patients remains dismal (5). Therefore, it is necessary to elucidate the pathogenic mechanism of colon cancer.

Recently, numerous studies have verified that the use of anesthetics during surgery may affect the progression of cancers (6). Sevoflurane is a commonly used inhaled anesthetic in clinical practice, which plays a vital role in the progression of various tumor cells. For example, Liang *et al* demonstrated that sevoflurane could suppress the metastasis of lung cancer cells (7). Gao *et al* revealed that sevoflurane suppressed the proliferation and metastasis of glioma cells (8). In the present study, the functions and mechanisms of sevoflurane in colon cancer were investigated.

Exosomes are discoid vesicles with a diameter of 50-140 nm (9). Exosomes secreted by tumor cells can transfer some tumor-specific biological information to neighboring cells or even distant cells and then promote the occurrence and development of tumors via delivering proteins, mRNAs, circular RNAs (circRNAs), microRNAs (miRNAs) and other bioactive substances (10,11). CircRNAs are a special class of non-coding RNAs (ncRNAs), which are characterized by closed ring structures (12). CircRNAs have emerged as crucial regulators in different types of cancers, including colon cancer. For example, Zhang *et al* revealed that circ-PIP5K1A was abnormally increased and could promote the progression of colon cancer by inducing cell viability and metastasis (13). Xu *et al* reported that circ_000984 served as an oncogene in colon cancer and circ_000984 knockdown hampered cell growth, metastasis and tumor formation (14). It has been reported that circRNA 3-hydroxy-3-methylglutaryl-CoA

synthase 1 (circ-HMGCS1) is associated with the progression of hepatoblastoma (HB) and colorectal cancer (CRC) (15, 16). However, the studies on circ-HMGCS1 in colon cancer remain limited.

miRNAs, a series of ncRNAs with approximately 22 nucleotides, mainly alter gene expression by recognizing the 3'-untranslated region (3'UTR) of target mRNAs (17). Multiple miRNAs have been confirmed to participate in the development of colon cancer via binding to target genes. For example, miR-28a-5p exerted its tumor-suppressive role in colon cancer by targeting CAMTA2 (18). miR-223-3p facilitated colon cancer cell growth and metastasis by binding to PRDM1 (19). miR-204-3p targeted HMGA2 to suppress cell viability and metastasis and facilitated cell apoptosis in colon cancer (20). Previous reports revealed that miR-34a-5p was reduced in CRC and the increase of miR-34a-5p suppressed tumor metastasis (21,22). Sphingosine-1-phosphate phosphatase 1 (SGPP1) has been demonstrated to promote cell growth and migration and hinder cell apoptosis in CRC (23). However, whether miR-34a-5p can target SGPP1 to take part in the regulation of colon cancer remains unclear.

The purpose of this research was to explore the functions of sevoflurane in colon cancer cell viability, apoptosis and invasion. In addition, the roles and potential mechanisms of exosomal circ-HMGCS1, miR-34a-5p and SGPP1 in colon cancer progression were investigated.

Materials and methods

Human serum collection. The serum samples were collected from 30 colon cancer patients (19 males and 11 females; age, 50-70 years) and 30 healthy volunteers (17 males and 13 females; age, 48-65 years) at the First Affiliated Hospital of Zhengzhou University from March 2015 to October 2017. The experiment was conducted following the approval that was obtained from the Ethics Committee of the First Affiliated Hospital of Zhengzhou University and written informed consents were signed by all participants. The collected samples were stored at -80˚C until use.

Cell culture. Two colon cancer cell lines (ATCC® CCL-228™, SW480; and ATCC® CCL-229, LOVO) were purchased from the American Type Culture Collection and a normal human colon mucosal epithelial cell line (C0972; NCM460) was obtained from Guandao Biological Company (https://www.biomart.cn/infosupply/37016225.htm). All cells were grown in Roswell Park Memorial Institute (RPMI)-1640 medium (cat. no. A1049101; Gibco; Thermo Fisher Scientific, Inc.) supplemented with 10% fetal bovine serum (cat. no. 16140063; FBS; Gibco; Thermo Fisher Scientific, Inc.) at an atmosphere of 5% CO_2 and 37˚C.

Sevoflurane treatment. SW480 and LOVO cells ($2x10^3$) at the exponential growth phase were seeded into plates and incubated overnight. Next, the plates were placed in an airtight glass chamber. Sevoflurane (product code YZ-1612540; Beijing Solarbio Science & Technology Co., Ltd.) was added into the chamber through an anesthetic vaporizer (BS-S6100 Plus; Guangzhou Bisen Medical Co., Ltd.). A gas monitor (PM8060; Drager) was employed to monitor the concentrations of sevoflurane. Cells were treated with various doses (1.7, 3.4 and 5.1%) of sevoflurane for 6 h, and then maintained in normal conditions for 24 h for further study. Cells without treatment were used as the control.

Cell transfection. The overexpression plasmid of circ-HMGCS1 (circ-HMGCS1) and its control (pcDNA), small interfering RNA targeting circ-HMGCS1 (si-circ-HMGCS1; 5'-TGGAAGCCUUGGGGCUUCGU-3') and its control (si-NC; 5'-UUCUCCGAACGUGUCACGUTT-3'), miR-34a-5p mimic (miR-34a-5p; 5'-GAUGGACGUGCUUGUCGUGAAAC-3') and its control (miR-NC; 5'-UUCUCCGAACGUGUCACGUTT-3'), miR-34a-5p inhibitor (anti-miR-34a-5p; 5'-CUACCUGCACCAACAGCACUU-3') and its control (anti-miR-NC; 5'-CAGUACUUUUGUGUAGUACAA-3'), lentivirus-mediated short hairpin against circ-HMGCS1 (sh-circ-HMGCS1; 5'-TTTGGGGCTTCGTGGGACACA-3') and its control (sh-NC; 5'-TTCTCCGAACGTGTCACGT-3') were synthesized by Shanghai GenePharma Co., Ltd. Cell transfection was carried out with the Lipofectamine 2000 reagent (cat. no. 11668019; Invitrogen; Thermo Fisher Scientific, Inc.).

3-(4,5-Dimethylthiazol-2-yl)-2,5-diphenyltetrazolium bromide (MTT) assay. The viability of SW480 and LOVO cells was assessed by MTT assay after relevant treatment. In brief, cells were seeded into 96-well plates at a density of $1x10^3$ cells/well and incubated overnight. Then 20 μl MTT (5 mg/ml; item no. IM0280; Beijing Solarbio Science & Technology Co., Ltd.) was added into each well after incubation for 24, 48 and 72 h followed by incubation for another 4 h at 37˚C. Next, dimethyl sulfoxide (DMSO; D8371; Beijing Solarbio Science & Technology Co., Ltd.) was added to dissolve the formazan crystals. The absorbance at 490 nm was determined using a microplate reader (Elx808™; BioTek Instruments, Inc.).

Flow cytometric assay. The Annexin V-fluorescein isothiocyanate (FITC)/propidium iodide (PI) Apoptosis Detection Kit (C1062M; Beyotime Institute of Biotechnology) was employed for the detection of cell apoptosis according to the instructions of manufacturers. In brief, SW480 and LOVO cells ($1x10^4$) were harvested and washed with phosphate-buffered saline (PBS; P1022; Beijing Solarbio Science & Technology Co., Ltd.) after relevant sevoflurane treatment and transfection. Then 5 μl Annexin V-FITC and 5 μl PI were added to stain cells for 15 min at room temperature in the dark. Finally, the rate of apoptotic cells was examined via a FACScan® flow cytometer (BD Biosciences) within 1 h and analyzed with software FlowJo (7.6.1; FlowJo LLC). The apoptotic rate was calculated as the sum of the early apoptosis rate and the late apoptosis rate.

Transwell assay. The invasion of SW480 and LOVO cells was tested using a Transwell insert (3379; 8 μm pore size; Corning Incorporated) which was pre-coated with Matrigel (product no. 356234; Beijing Solarbio Science & Technology Co., Ltd.). Cells ($1x10^4$) in serum-free RPMI-1640 medium were added into the upper chamber. RPMI-1640 medium supplemented with 10% FBS was added into the bottom chamber. After 48 h, cells remaining on the upper chamber were removed and the cells that invaded to the lower surface

were fixed with 70% methanol for 30 min at room temperature and stained with 0.1% crystal violet (IC0600; Beijing Solarbio Science & Technology Co., Ltd.) for 15 min at room temperature. The number of invaded cells was analyzed under a light microscope (Olympus Corporation) at a magnification of x100.

Western blot analysis. After being extracted from serums, cells and exosomes using RIPA buffer (P0013C; Beyotime Institute of Biotechnology), total protein (20 μg) was quantified by a BCA Protein Quantification Kit (E112-01/02; Vazyme) and then separated through 10% sodium dodecyl sulfonate-polyacrylamide gel (SDS-PAGE; P1200; Beijing Solarbio Science & Technology Co., Ltd.). Then the proteins were transferred onto polyvinylidene difluoride membranes (PVDF; 3010040001; EMD Millipore) and blocked in 5% skim milk for 2 h at room temperature. Next, the membranes were incubated with primary antibodies against cyclin D1 (product code ab16663; 1:200), p21 (product code ab109199; 1:1,000), matrix metallopeptidase 9 (MMP9; product code ab38898; 1:1,000), CD9 (product code ab92726; 1:2,000), CD63 (product code ab68418; 1:2,000), SGPP1 (product code ab108435; 1:2,000), GAPDH (product code ab181602; 1:5,000) or β-actin (product code ab8227; 1:5,000; all from Abcam) overnight at 4˚C and secondary antibody goat anti-rabbit IgG H&L (product code ab150077; 1:5,000; Abcam) for 2 h at room temperature. Finally, the protein bands were visualized by an enhanced chemiluminescence reagent (E411-03/04/05; Vazyme) and analyzed by ImageJ software (v1.8.0; National Institutes of Health).

Exosome isolation. The serum-exosomes were isolated with ExoQuick precipitation kit (EXOQ5A-1; System Biosciences) according to the manufacturer's instructions. Briefly, ExoQuick solution was added into the serum samples and incubated for 30 min at 4˚C. Then the mix was centrifuged for 30 min at 1,500 x g at room temperature. Subsequently, the supernatant was carefully removed and then centrifuged for 5 min at 1,500 x g to remove the extra liquid. Exosome pellets were resuspended in PBS (P1022; Beijing Solarbio Science & Technology Co., Ltd.) and preserved at -80˚C. Exosomes were isolated from cultured cells through differential ultracentrifugation as previously described (24).

Transmission electron microscopy (TEM). Exosome pellets were suspended in PBS (P1022; Beijing Solarbio Science & Technology Co., Ltd.) and then fixed with 4% paraformaldehyde (E672002; Shanghai Sangon Biotech Co., Ltd.) overnight at 4˚C and 4% glutaraldehyde (A600875; Shanghai Sangon Biotech Co., Ltd.) for 30 min at 4˚C in phosphate buffer (pH 7.4), and maintained overnight at 4˚C until the TEM assay. The exosomes were placed on a 400-mesh carbon-coated copper grid and stained with 2% phosphotungstic acid solution (pH 7.0; G1599; Solarbio) for 2 min at room temperature. The morphologies of the samples were examined with a JEM-1200EX transmission electron microscope (JEOL, Ltd.) at the magnification of x50,000.

Nanoparticle tracking analysis (NTA). The size of the exosomes was examined using the Nanosight NS 300 system (NanoSight Technology) according to the manufacturer's instructions.

Reverse transcription-quantitative polymerase chain reaction (RT-qPCR). Total RNA was extracted from serums, cells and exosomes with TRIzol reagent (15596018; Invitrogen; Thermo Fisher Scientific, Inc.). Then reverse transcription was conducted using High Capacity cDNA Reverse Transcription Kit (4368814; Applied Biosystems; Thermo Fisher Scientific, Inc.) or miRNA 1st Strand cDNA Synthesis Kit (MR101-01/02; Vazyme) according to the manufacturer's instructions. Subsequently, RT-qPCR was conducted using AceQ Universal SYBR qPCR Master Mix (Q511-02; Vazyme) on an ABI 7500 PCR system (4351104; Applied Biosystems; Thermo Fisher Scientific, Inc.) under the thermocycling conditions: i) Initial denaturation at 95˚C for 5 min; ii) 40 cycles of 95˚C for 10 sec and 60˚C for 30 sec; iii) 95˚C for 15 sec, 60˚C for 60 sec and 95˚C for 15 sec. The expression was analyzed with the $2^{-\Delta\Delta Cq}$ method (25). Glyceraldehyde 3-phosphate dehydrogenase (GAPDH) or U6 was used as an internal control. The primer sequences were listed as follows: circ-HMGCS1 forward, 5'-TCTAGCTCGGATGTTGCTGA-3' and reverse, 5'-TCAGGCTTGTAAAAATCATAGGC-3'; miR-34a-5p forward, 5'-CTGGGAGGTGGCAGTGTCTTAGC-3' and reverse, 5'-TCAACTGGTGTCGTGGAGTCGG-3'; SGPP1 forward, 5'-TGGTCCTCCTCACCTATGGC-3' and reverse, 5'-CTAGAGAACACCAGCAGGGA-3'; GAPDH forward, 5'-CCGGGAAACTGTGGCGTGATGG-3' and reverse, 5'-AGGTGGAGGAGTGGGTGTCGCTGTT-3'; U6 forward, 5'-TGCGGGTGCTCGCTTCGGCAGC-3' and reverse, 5'-CCAGTGCAGGGTCCGAGGT-3'.

Dual-luciferase reporter assay. The potential binding sites between miR-34a-5p and circ-HMGCS1 or SGPP1 were predicted by starBase v2.0 (http://starbase.sysu.edu.cn/index.php) and verified by dual-luciferase reporter assay. The fragments of circ-HMGCS1 or 3'UTR of SGPP1 containing the predicted wild-type or mutant miR-34a-5p binding sequences were cloned into the pmirGLO vector (E1330; Promega Corporation) to construct luciferase reporter plasmids WT-circ-HMGCS1, MUT-circ-HMGCS1, SGPP1 3'UTR-WT and SGPP1 3'UTR-MUT, respectively. Then miR-34a-5p or miR-NC was transfected into SW480 or LOVO cells along with relevant plasmid. Dual-Luciferase Reporter Assay Kit (E1910; Promega Corporation) was used to detect the luciferase activity according to the manufacturer's instructions. The *Renilla* luciferase activity was normalized to firefly luciferase activity.

RNA immunoprecipitation (RIP) assay. Magna RIP RNA Binding Protein Immunoprecipitation Kit (17-700; EMD Millipore) was used to conduct RIP assays. Briefly, SW480 and LOVO cells were lysed in RIP buffer and then incubated overnight with magnetic beads coated with antibody against Argonaute2 (Anti-Ago2; product code ab32381; 1:2,000; Abcam) or immunoglobulin G (Anti-IgG; product code ab109489; 1:5,000; Abcam) at 4˚C. Subsequently, the samples were washed and incubated with proteinase K (P9460; Beijing Solarbio Science & Technology Co., Ltd.) at 55˚C for 30 min to isolate the RNA-protein complexes from beads. Finally, RNAs in the magnetic complexes were extracted and the enrichment of circ-HMGCS1, miR-34a-5p and SGPP1 was analyzed via RT-qPCR.

Murine xenograft model. A total of 24 male nude mice (17-23 g) were purchased from Shanghai SLAC Laboratory Animals Co., Ltd and divided into 3 groups (n=8/group): sh-NC, sh-NC+SEV and sh-circ-HMGCS1+SEV. All the mice were housed in a pathogen-free condition at 28˚C and 45% humidity with a 12-h light/dark cycle and fed sterile fodder and drinking water. After being transfected with sh-circ-HMGCS1 or sh-NC for 48 h and treated with 5.1% sevoflurane for 6 h, $4x10^6$ SW480 cells were cultured overnight and then subcutaneously inoculated into the right forelimb of the nude mice. After 7 days, the mice were administered with sevoflurane every 4 days and the tumor weight was monitored concurrently. The tumor weight was calculated with the formula: (length x $width^2$)/2. Subsequently, 27 days later, the mice were sacrificed by cervical dislocation. The criteria for confirming the death of the mice were absence of breathing for 2-3 min and absence of blink reflex. Tumors were collected and weighted. The collected tumor samples were stored at -80˚C. The experiment was approved by the Ethics Committee of Animal Research of the First Affiliated Hospital of Zhengzhou University. The mice with tumors were monitored daily for proper treatment and for signs of convulsions, self-injury, dyspnea and other phenomena, where corresponding countermeasures would be taken. The humane endpoints of the animal studies were as follows: A tumor burden greater than 10% body weight and a tumor that did not exceed 20 mm in any one dimension. The maximal tumor volume in our experiments was 960 mm^3.

Statistical analysis. The data collected from three independent experiments were displayed as the mean ± standard deviation (SD), and processed by using software GraphPad Prism 7 (GraphPad Software, Inc.). Paired Student's *t*-test or one-way analysis of variance (ANOVA) followed by Tukey's test was applied to compare differences among groups. The correlations between the expression of miR-34a-5p and circ-HMGCS1, as well as miR-34a-5p and SGPP1 were analyzed using Spearman's correlation coefficient analysis. A P-value <0.05 was considered to indicate a statistically significant difference.

Results

Sevoflurane suppresses cell viability and invasion and facilitates cell apoptosis in colon cancer cells. In order to explore the function of sevoflurane in the progression of colon cancer, SW480 and LOVO cells were treated with various concentrations (1.7, 3.4 and 5.1%) of sevoflurane and then cell viability, apoptosis and invasion were investigated. The data of the MTT assay indicated that compared to control group, cell viability was significantly suppressed by sevoflurane in a concentration-dependent manner in both SW480 and LOVO cells (Fig. 1A and B). Flow cytometric analysis revealed that the apoptosis of SW480 and LOVO cells was significantly promoted by the treatment of sevoflurane compared to control group (Fig. 1C). The number of invaded cells was significantly reduced in a dose-dependent manner in SW480 and LOVO cells by sevoflurane treatment compared with the control group, as determined by Transwell assays (Fig. 1D). In addition, the protein levels of cyclin D1, p21 and MMP9 in SW480 and LOVO cells treated with sevoflurane were measured via western blotting. The data revealed that cyclin D1 and MMP9 were decreased while p21 was increased in a concentration-dependent manner in SW480 and LOVO cells after sevoflurane treatment (Fig. 1E and F). Collectively, the data indicated that sevoflurane could inhibit the progression of colon cancer cells.

Exosomal circ-HMGCS1 is increased and cytoplasm miR-34a-5p is decreased in the serums and cells of colon cancer patients. To analyze the function of circ-HMGCS1 packaged in exosomes, serum derived from colon cancer patients and colon cancer cell-derived exosomes were first isolated. Then the morphology of particles isolated from the serums of the patients was observed by TEM. It was observed that the particles exhibited typical lipid bilayer membrane-encapsulated nanoparticles (Fig. 2A). The data of the western blot assay revealed that the markers of exosomes (CD9 and CD63) could be detected in the serums of the colon cancer patients and in the colon cancer cell-derived particles (Fig. 2B). The NTA assay revealed that the diameters of the particles isolated from the serums of the patients were 80-130 nm (Fig. 2C). These data indicated that the isolated particles were exosomes. Subsequently, the expression of circ-HMGCS1 in the exosomes was assessed by RT-qPCR. The data revealed that circ-HMGCS1 was expressed at a higher level in the exosomes from the serums of colon cancer patients and colon cancer cells (SW480 and LOVO cells) compared to the exosomes derived from normal serums and NCM460 cells (Fig. 2D and E). In addition, the expression of miR-34a-5p in the serums of colon cancer patients and colon cancer cells was examined. As revealed in Fig. 2F and G, miR-34a-5p was downregulated in the serums of colon cancer patients and colon cancer cells compared to normal serums and cells. There was an inverse correlation between circ-HMGCS1 and miR-34a-5p in the serums of patients with colon cancer, as analyzed by Spearman's correlation coefficient analysis (Fig. 2H). Collectively, the aberrant expression of circ-HMGCS1 and miR-34a-5p may be involved in the progression of colon cancer.

Overexpression of circ-HMGCS1 abrogates the effects of sevoflurane on cell viability, apoptosis and invasion in colon cancer cells. In order to confirm whether circ-HMGCS1 was involved in the progression of colon cancer cells, SW480 and LOVO cells were treated with various concentrations (1.7, 3.4 and 5.1%) of sevoflurane. Then the effect of sevoflurane on circ-HMGCS1 expression was determined by RT-qPCR. The data revealed that sevoflurane treatment led to a significant reduction of circ-HMGCS1 in a dose-dependent manner in SW480 and LOVO cells (Fig. 3A). SW480 and LOVO cells exposed to a concentration of 5.1% SEV were used for the subsequent functional experiments due to the stronger suppression in circ-HMGCS1 expression. Subsequently, SW480 and LOVO cells were transfected with pcDNA or circ-HMGCS1 and then exposed to 5.1% SEV for 6 h. As revealed in Fig. 3B, the downregulation of circ-HMGCS1 in SW480 and LOVO cells caused by sevoflurane exposure was partly reversed by the administration of circ-HMGCS1. An MTT assay revealed that the inhibitory effect on cell viability mediated by sevoflurane was effectively abolished by the overexpression of

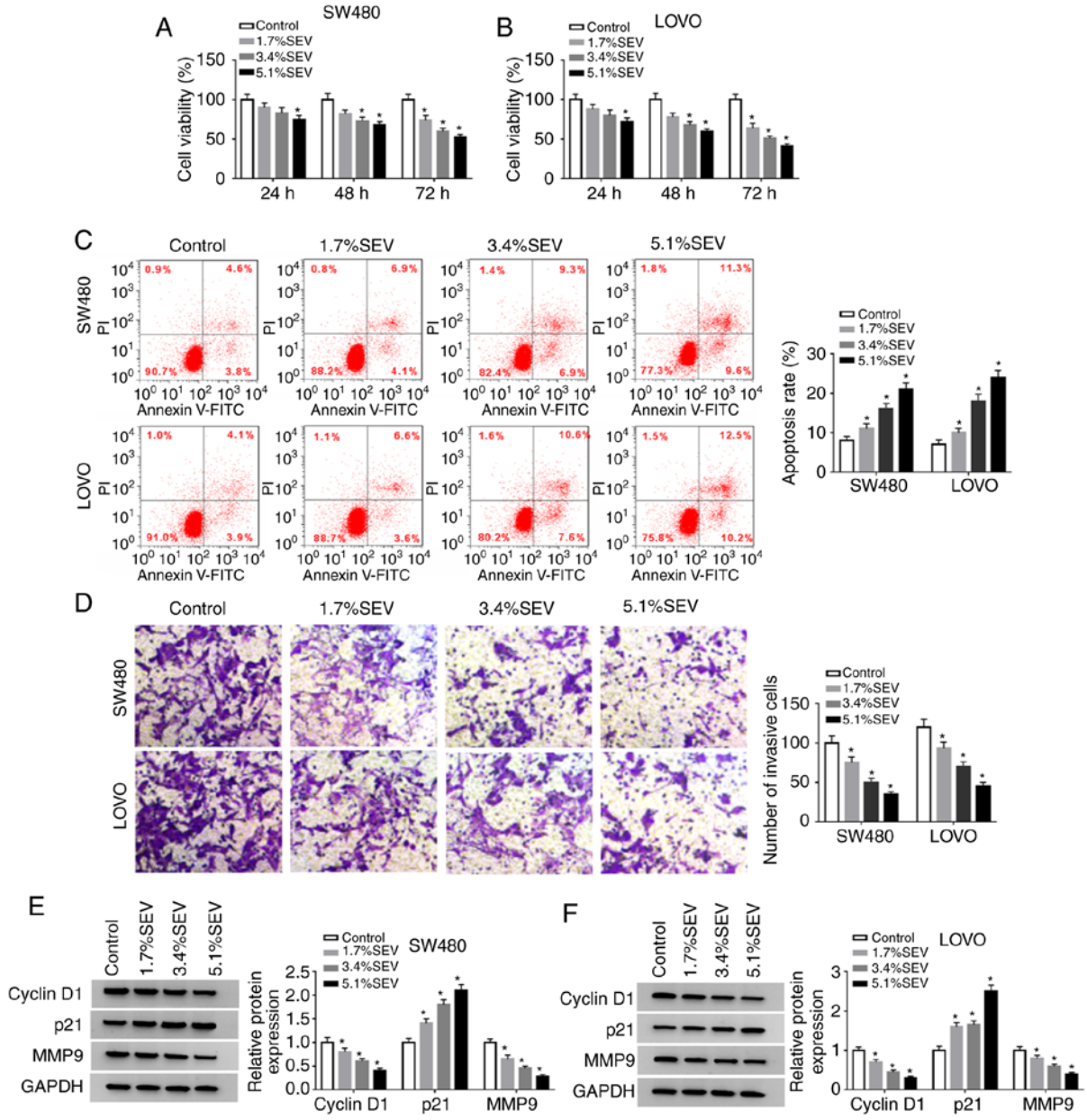

Figure 1. Sevoflurane inhibits cell viability and invasion and induces cell apoptosis in colon cancer cells. SW480 and LOVO cells were divided into 4 groups: Control, 1.7% SEV, 3.4% SEV and 5.1% SEV. (A and B) The viability of SW480 and LOVO cells was determined by MTT assay. (C) The apoptosis of SW480 and LOVO cells was analyzed by flow cytometric analysis. (D) The invasion of SW480 and LOVO cells was evaluated via Transwell assay. (E and F) The protein levels of cyclin D1, p21 and MMP9 were assessed via western blotting. *P<0.05 vs. the control group. SEV, sevoflurane; MMP9, matrix metallopeptidase 9.

circ-HMGCS1 in both SW480 and LOVO cells (Fig. 3C and D). As revealed by flow cytometric analysis, the apoptosis of SW480 and LOVO cells was facilitated by the treatment of sevoflurane, while circ-HMGCS1 overexpression reversed this effect (Fig. 3E). Transwell assay data indicated that sevoflurane treatment resulted in a significant suppression in cell invasion in SW480 and LOVO cells, however, circ-HMGCS1 overexpression abolished this suppression (Fig. 3F). Western blot analysis revealed that sevoflurane treatment decreased the levels of cyclin D1 and MMP9 and increased the level of p21 in SW480 and LOVO cells, whereas the effects were rescued by circ-HMGCS1 (Fig. 3G and H). To sum up, circ-HMGCS1 promoted sevoflurane-mediated proliferation and invasion and suppressed sevoflurane-mediated apoptosis in colon cancer cells.

Circ-HMGCS1 silencing suppresses cell viability and invasion and promotes cell apoptosis by targeting miR-34a-5p in colon cancer cells. Since circ-HMGCS1 and miR-34a-5p were dysregulated in colon cancer patients, it was theorized that miR-34a-5p may be a target of circ-HMGCS1. By searching the online website starBase v2.0, it was revealed that miR-34a-5p contained the complementary sequences of circ-HMGCS1 (Fig. 4A). Next, dual-luciferase reporter and RIP assays were conducted. The dual-luciferase reporter assay revealed that compared to miR-NC and WT-circ-HMGCS1 co-transfected groups, the luciferase activity in SW480 and LOVO cells co-transfected with miR-34a-5p and WT-circ-HMGCS1 was inhibited, whereas no change was observed in MUT-circ-HMGCS1 groups (Fig. 4B and C). The RIP assay revealed that miR-34a-5p and circ-HMGCS1 combined to an

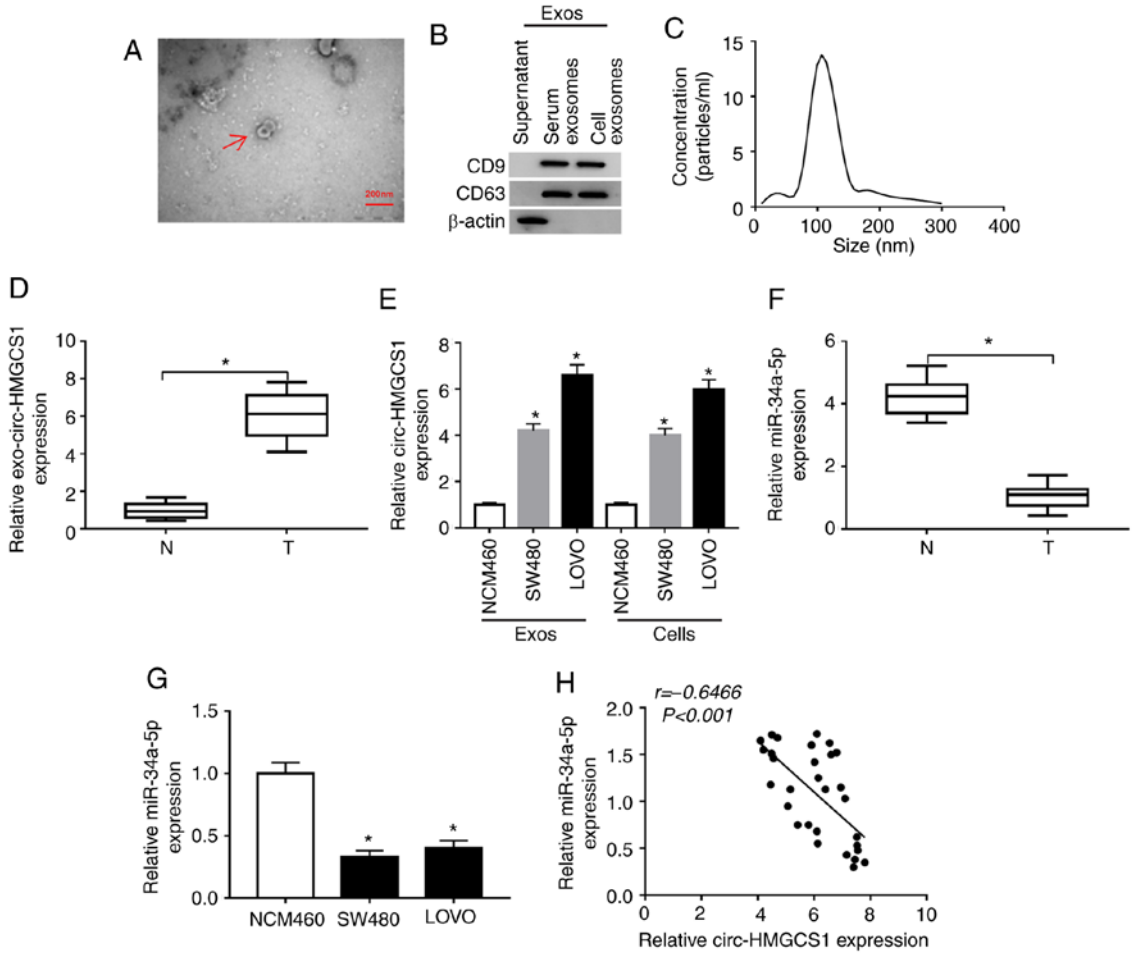

Figure 2. Upregulation of exosomal circ-HMGCS1 and downregulation of miR-34a-5p in the serums of colon cancer patients and colon cancer cells. (A) The morphology of exosomes derived from the serums of patients was observed by TEM analysis. (B) Exosomal markers (CD9 and CD63) were detected by western blotting. (C) The size distribution of exosomes derived from the serums of patients was analyzed by NTA. (D) The expression of circ-HMGCS1 in the exosomes derived from the serums of colon cancer patients (Tumor group) and healthy volunteers (Normal group) was determined by RT-qPCR. (E) The expression levels of exosomal circ-HMGCS1 and cytoplasm circ-HMGCS1 in NCM460, SW480 and LOVO cells were measured by RT-qPCR. The expression of miR-34a-5p in (F) the serums of colon cancer patients, and (G) colon cancer cells and corresponding controls was examined by RT-qPCR. (H) The correlation between circ-HMGCS1 and miR-34a-5p was analyzed via Spearman's correlation coefficient analysis. *P<0.05 vs. the normal group or the NCM460 group. circ-HMGCS1, circular RNA 3-hydroxy-3-methylglutaryl-CoA synthase 1; miR, microRNA; TEM, transmission electron microscopy; NTA, nanoparticle tracking analysis; RT-qPCR, reverse transcription-quantitative polymerase chain reaction.

Ago2 immunoprecipitation complex were both significantly enriched compared to the IgG group in SW480 and LOVO cells (Fig. 4D and E). As revealed in Fig. 4F and G, si-circ-HMGCS1 transfection led to a significant decrease in circ-HMGCS1 expression and a significant increase in miR-34a-5p expression in SW480 and LOVO cells, while circ-HMGCS1 transfection exhibited the opposite results. To further explore the association between circ-HMGCS1 and miR-34a-5p in the progression of colon cancer cells, SW480 and LOVO cells were transfected with si-NC, si-circ-HMGCS1, si-circ-HMGCS1+anti-miR-NC or si-circ-HMGCS1+anti-miR-34a-5p. It was revealed that the upregulation of miR-34a-5p caused by circ-HMGCS1 silencing was reversed following the inhibition of miR-34a-5p (Fig. 4H). Furthermore, circ-HMGCS1 deficiency resulted in a significant suppression in cell viability and invasion and a significant promotion in cell apoptosis, while these influences were all weakened by miR-34a-5p inhibition in SW480 and LOVO cells (Fig. 4I-L). In addition, the levels of cyclin D1 and MMP9 were reduced and the level of p21 was increased in SW480 and LOVO cells transfected with si-circ-HMGCS1; however, inhibitors of miR-34a-5p abolished the effects (Fig. 4M and N). Collectively, miR-34a-5p inhibition alleviated the inhibitory effect of circ-HMGCS1 knockdown on colon cancer cell progression.

miR-34a-5p inhibition alleviates sevoflurane-mediated effects on cell viability, apoptosis and invasion in colon cancer cells. To further reveal the underlying mechanism of sevoflurane in the development of colon cancer, the effect of sevoflurane on miR-34a-5p expression was investigated. The data revealed that miR-34a-5p was significantly increased following the treatment of sevoflurane in a dose-dependent manner (Fig. 5A). Then anti-miR-34a-5p or anti-miR-NC was transfected into SW480 and LOVO cells and then these cells were exposed to 5.1% SEV. It was observed that sevoflurane-mediated upregulation in miR-34a-5p was partially reversed by the transfection of anti-miR-34a-5p (Fig. 5B). Moreover, the suppressive effects of sevoflurane on cell viability (Fig. 5C and D) and cell invasion (Fig. 5F) and the promoting effect on cell apoptosis (Fig. 5E) were all weakened following miR-34a-5p inhibition

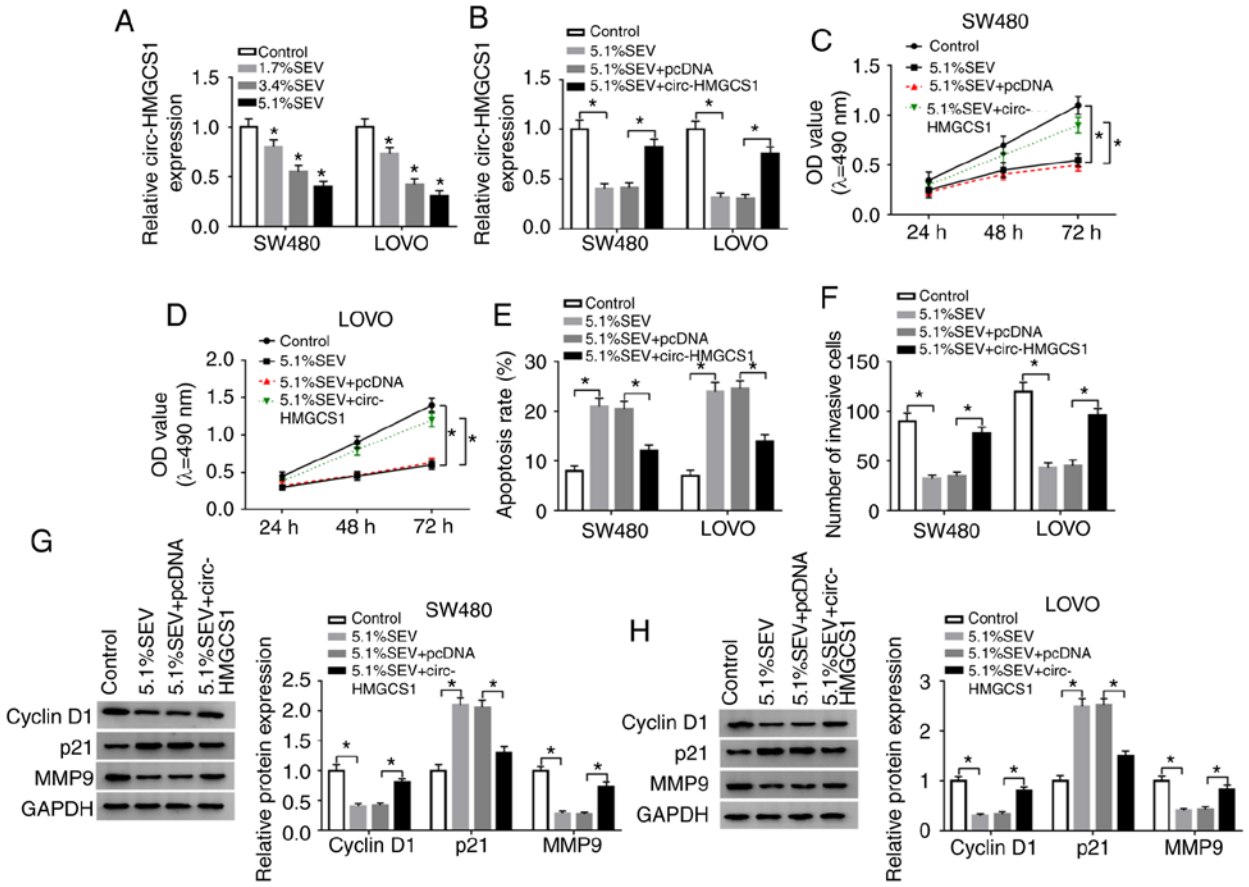

Figure 3. Sevoflurane suppresses cell viability and invasion and promotes cell apoptosis by downregulating circ-HMGCS1 in colon cancer cells. (A) The expression of circ-HMGCS1 in SW480 and LOVO cells untreated (control) or treated with 1.7% SEV, 3.4% SEV or 5.1% SEV was determined by RT-qPCR. (B-H) SW480 and LOVO cells were assigned to Control, 5.1% SEV, 5.1% SEV+pcDNA and 5.1% SEV+circ-HMGCS1 groups. (B) The expression of circ-HMGCS1 in SW480 and LOVO cells was examined by RT-qPCR. (C and D) The viability of SW480 and LOVO cells was assessed using MMT assay. (E) The apoptosis of SW480 and LOVO cells was evaluated by flow cytometric analysis. (F) The invasion of SW480 and LOVO cells was examined using Transwell assay. (G and H) The protein levels of cyclin D1, p21 and MMP9 were determined via western blot assay. *P<0.05 vs. the control or the 5.1% SEV+pcDNA group. circ-HMGCS1, circular RNA 3-hydroxy-3-methylglutaryl-CoA synthase 1; SEV, sevoflurane; RT-qPCR, reverse transcription-quantitative polymerase chain reaction; MMP9, matrix metallopeptidase 9; OD, optical density.

in SW480 and LOVO cells. As indicated by western blot analysis, miR-34a-5p inhibition effectively rescued the reduction in cyclin D1 and MMP9 expression and the increase in p21 expression caused by sevoflurane in SW480 and LOVO cells (Fig. 5G and H). These data indicated that the influence of sevoflurane on cell progression was restored by miR-34a-5p depletion in colon cancer.

SGPP1 is a target gene of miR-34a-5p. By further searching online software starBase v2.0, it was revealed that the 3'UTR of SGPP1 contained the putative binding sites of miR-34a-5p (Fig. 6A). Dual-luciferase reporter assays revealed that co-transfection of miR-34a-5p and SGPP1 3'UTR-WT led to a significant suppression in the luciferase activity in SW480 and LOVO cells compared with miR-NC and SGPP1 3'UTR-WT co-transfected cells, while the luciferase activity was not affected in the SGPP1 3'UTR-MUT groups (Fig. 6B and C). RIP assays indicated that miR-34a-5p and SGPP1 levels were increased in SW480 and LOVO cells after Ago2 RIP compared to the IgG control group (Fig. 6D and E). As anticipated, the mRNA and protein levels of SGPP1 in the serums of colon cancer patients were markedly increased compared to those in the serums of healthy volunteers (Fig. 6F and G). Similarly, the protein level of SGPP1 was increased in SW480 and LOVO cells compared to NCW460 cells (Fig. 6H). Moreover, SGPP1 expression was negatively correlated with miR-34a-5p expression in the serums of colon cancer patients (Fig. 6I). As revealed in Fig. 6J-L, miR-34a-5p transfection significantly enhanced miR-34a-5p expression and decreased SGPP1 protein expression in SW480 and LOVO cells, while anti-miR-34a-5p transfection exhibited the opposite results. Collectively, miR-34a-5p negatively modulated SGPP1 expression by directly targeting SGPP1 in colon cancer cells.

Sevoflurane suppresses SGPP1 expression via the circ-HMGCS1/miR-34a-5p axis in colon cancer cells. To investigate the relationship among sevoflurane, circ-HMGCS1, miR-34a-5p and SGPP1 in colon cancer cells, SW480 and LOVO cells were transfected with si-NC, si-circ-HMGCS1, si-circ-HMGCS1+anti-miR-NC or si-circ-HMGCS1+anti-miR-34a-5p. The data revealed that circ-HMGCS1 knockdown decreased the expression of SGPP1 in both SW480 and LOVO cells, while miR-34a-5p inhibition partly restored the effect, indicating that circ-HMGCS1 could suppress SGPP1 expression via sponging miR-34a-5p (Fig. 7A and C). In addition, it was revealed that sevoflurane

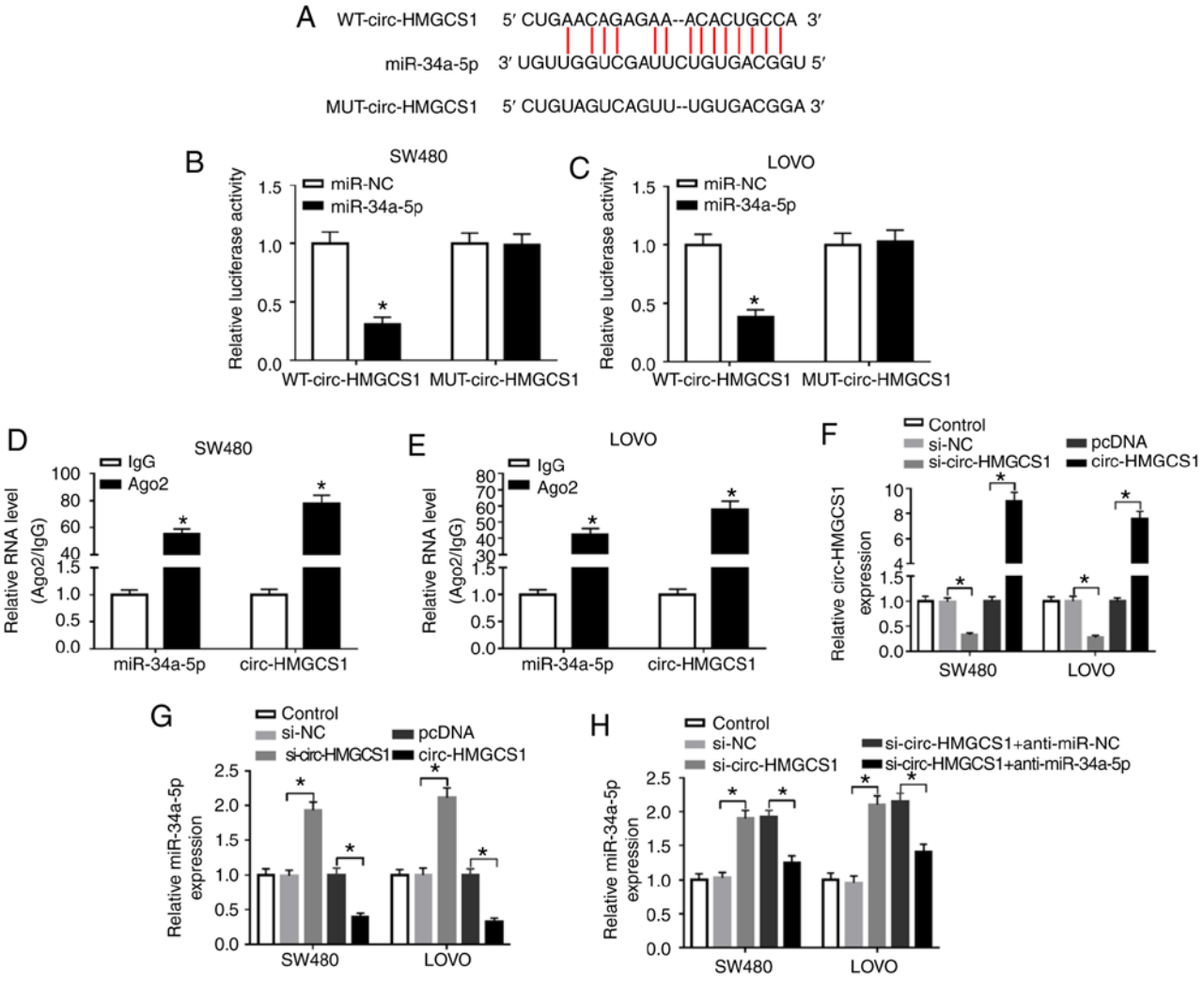

Figure 4. miR-34a-5p downregulation reverses the effects of circ-HMGCS1 silencing on cell viability, apoptosis and invasion in colon cancer cells. (A) The potential binding sequences between circ-HMGCS1 and miR-34a-5p. (B and C) A dual-luciferase reporter assay was conducted to verify the association between circ-HMGCS1 and miR-34a-5p. *P<0.05 vs. the miR-NC group. (D and E) The enrichment of miR-34a-5p and circ-HMGCS1 combined to Ago2/IgG precipitation complexes was determined by RT-qPCR. *P<0.05 vs. the IgG group. (F and G) The levels of circ-HMGCS1 and miR-34a-5p in SW480 and LOVO cells transfected with si-NC, si-circ-HMGCS1, pcDNA or circ-HMGCS1 were measured by RT-qPCR. *P<0.05 vs. the si-NC group or the pcDNA group. (H) SW480 and LOVO cells were divided into 5 groups: Control, si-NC, si-circ-HMGCS1, si-circ-HMGCS1+anti-miR-NC and si-circ-HMGCS1+anti-miR-34a-5p. (H) The expression of miR-34a-5p was measured by RT-qPCR. *P<0.05 vs. the si-NC group or the si-circ-HMGCS1+anti-miR-NC group.

treatment caused a significant decrease in SGPP1 expression in SW480 and LOVO cells, however circ-HMGCS1 overexpression reversed the decrease (Fig. 7B and D). Collectively the results demonstrated that sevoflurane could modulate SGPP1 expression via circ-HMGCS1/miR-34a-5p axis.

Circ-HMGCS1 knockdown suppresses tumorigenesis of colon cancer in vivo. To reveal the effect of circ-HMGCS1 in tumor progression *in vivo*, SW480 cells were stably transfected with sh-circ-HMGCS1 or sh-NC and then stimulated with sevoflurane. As revealed in Fig. 8A, sh-circ-HMGCS1 transfection significantly reduced the expression level of circ-HMGCS1 in SW480 cells compared to the sh-NC group, indicating the successful transfection of sh-circ-HMGCS1. Then, SW480 cells were injected into the nude mice to establish a murine xenograft model. It was revealed that the tumor volume and tumor weight were decreased by circ-HMGCS1 knockdown (Fig. 8B and C). Subsequently, the levels of circ-HMGCS1, miR-34a-5p and SGPP1 were determined in the collected tumors. The data revealed that circ-HMGCS1 and SGPP1 levels were significantly decreased and the level of miR-34a-5p was significantly increased in the tumors collected from the sh-circ-HMGCS+SEV group compared to that in the sh-NC+SEV group (Fig. 8D-F). These results demonstrated that silencing of circ-HMGCS1 could block tumor growth of colon cancer *in vivo*.

Based on all the experimental results, we arrived at the conclusion that sevoflurane treatment could inhibit the circHMGCS1/miR-34a-5p/SGPP1 axis, thereby suppressing colon cancer cell growth and metastasis (Fig. 8G).

Discussion

Emerging evidence has revealed that anesthetic techniques or drugs can affect the development of human cancers (26). In the present study, the function and underlying mechanisms of sevoflurane in colon cancer progression were explored and it was demonstrated that sevoflurane suppressed colon cancer

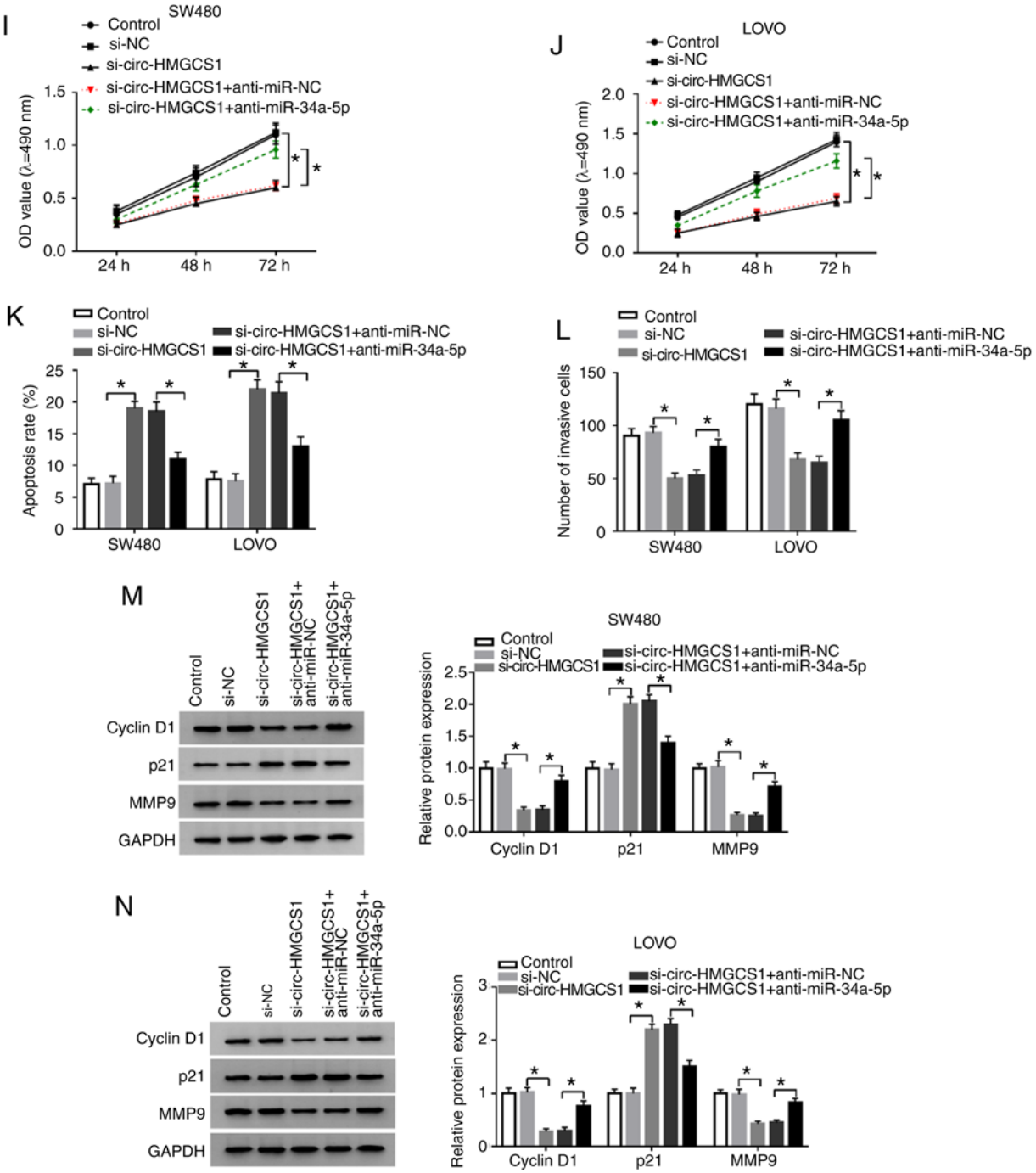

Figure 4. Continued. (I and J) Cell viability, (K) apoptosis and (L) invasion were evaluated by MTT assay, flow cytometric analysis and Transwell assay, respectively. (M and N) The levels of cyclin D1, p21 and MMP9 in SW480 and LOVO cells were examined using western blotting. *P<0.05 vs. the si-NC group or the si-circ-HMGCS1+anti-miR-NC group. miR, microRNA; circ-HMGCS1, circular RNA 3-hydroxy-3-methylglutaryl-CoA synthase 1; Ago2, Argonaute2; IgG, immunoglobulin G; RT-qPCR, reverse transcription-quantitative polymerase chain reaction; si, small interfering; NC, negative control; MMP9, matrix metallopeptidase 9; WT, wild-type; MUT, mutated.

cell viability and invasion and facilitated apoptosis via regulating the circ-HMGCS1/miR-34a-5p/SGPP1 axis.

Sevoflurane exerts a tumor-suppressive role in colon cancer, as demonstrated by former studies. For example, Yang *et al* revealed that sevoflurane suppressed cell viability and motility and induced cell apoptosis and autophagy in colon cancer (27). Fan *et al* demonstrated that sevoflurane led to an evident suppression of CRC cell metastasis in a dose-dependent manner (28). Consistently, we observed that sevoflurane hindered colon cancer cell viability and invasion and contributed to apoptosis in a concentration-dependent manner.

Subsequently, the potential mechanisms of sevoflurane in colon cancer were explored. It was determined that exosomal circ-HMGCS1 was increased in the serums of colon cancer patients and colon cancer cells. Moreover, cytoplasm circ-HMGCS1 was increased in colon cancer cells. These data indicated that circ-HMGCS1 may be a diagnostic and prognostic biomarker for patients with colon cancer. Furthermore, the effect of sevoflurane on circ-HMGCS1 expression

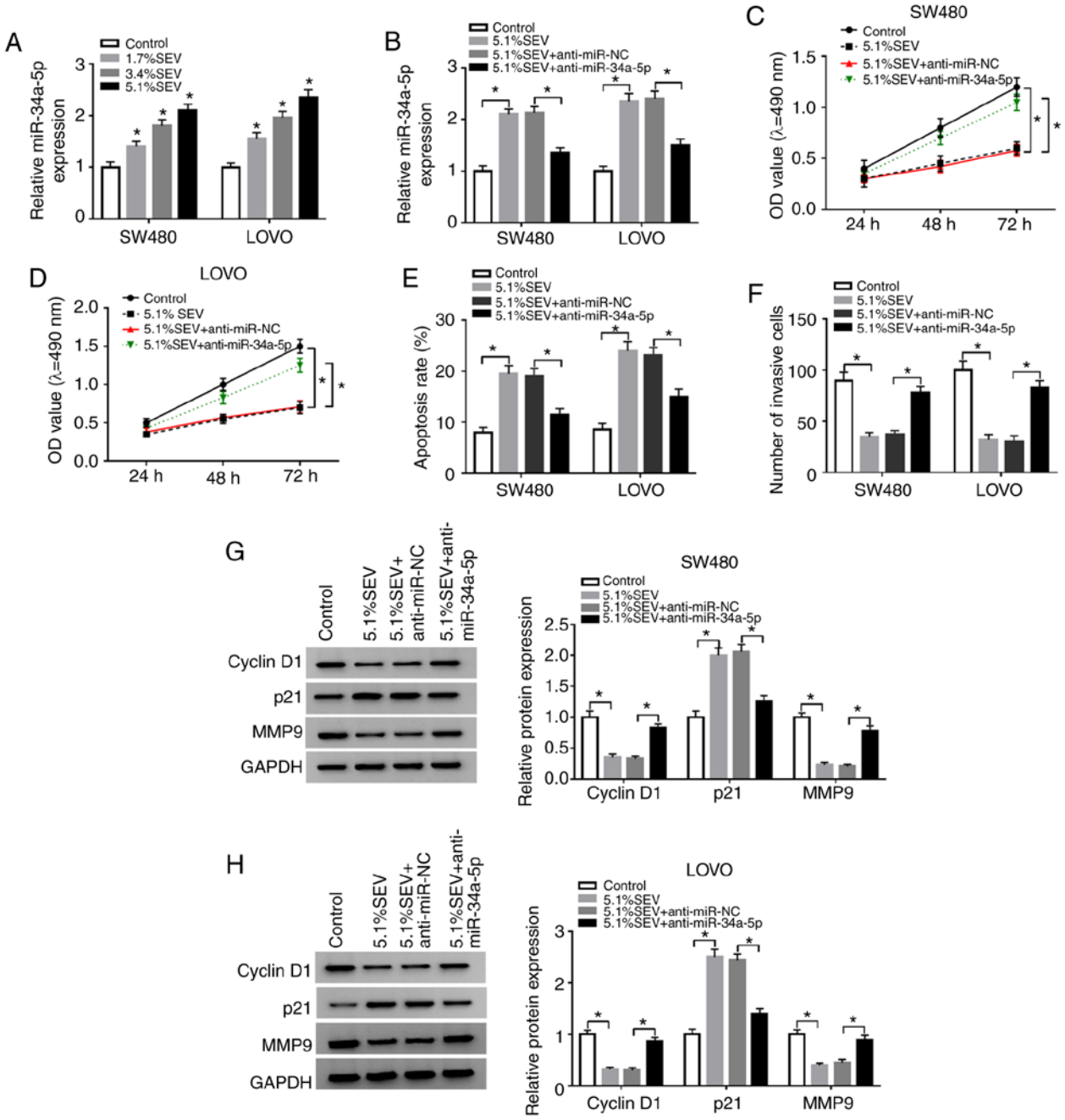

Figure 5. Effects of sevoflurane on cell viability, apoptosis and invasion are reversed by miR-34a-5p inhibition in colon cancer cells. (A) SW480 and LOVO cells were exposed to various concentrations (1.7, 3.4 and 5.1%) of sevoflurane and then miR-34a-5p expression was detected by RT-qPCR. (B-H) SW480 and LOVO cells were divided into 4 groups: Control, 5.1% SEV, 5.1% SEV+anti-miR-NC and 5.1% SEV+anti-miR-34a-5p. (B) miR-34a-5p expression in SW480 and LOVO cells was measured by RT-qPCR. (C and D) The viability, (E) apoptosis and (F) invasion of SW480 and LOVO cells were analyzed via MTT assay, flow cytometric analysis and Transwell assay, respectively. (G and H) The protein levels of cyclin D1, p21 and MMP9 were determined using western blotting. *P<0.05 vs. the control group or the 5.1% SEV+anti-miR-NC group. miR, microRNA; RT-qPCR, reverse transcription-quantitative polymerase chain reaction; SEV, sevoflurane; NC, negative control; MMP9, matrix metallopeptidase 9; OD, optical density.

was explored and it was revealed that circ-HMGCS1 was suppressed by sevoflurane treatment in a dose-dependent manner. Zhen *et al* demonstrated that circ-HMGCS1 was significantly increased in HB and circ-HMGCS1 deficiency hindered cell growth and facilitated cell apoptosis *in vitro* and blocked tumorigenesis *in vivo* (15). Dong *et al* revealed that the increase of circ-HMGCS1 predicted a poor prognosis and circ-HMGCS1 silencing inhibited cell growth and promoted apoptosis in CRC (16). In the present study, the effects on cell viability, apoptosis and invasion mediated by sevoflurane were abolished by the overexpression of circ-HMGCS1 in colon cancer, indicating that circ-HMGCS1 overexpression could enhance colon cancer cell viability and invasion and suppress apoptosis. Moreover, circ-HMGCS1 silencing could hinder tumor growth *in vivo*. All these data demonstrated that exosome-transmitted circ-HMGCS1 functioned as an oncogene in colon cancer.

CircRNAs contain the binding sites of miRNAs and act as sponges of miRNAs to regulate gene transcription (29,30). Herein, miR-34a-5p was identified as a direct target of

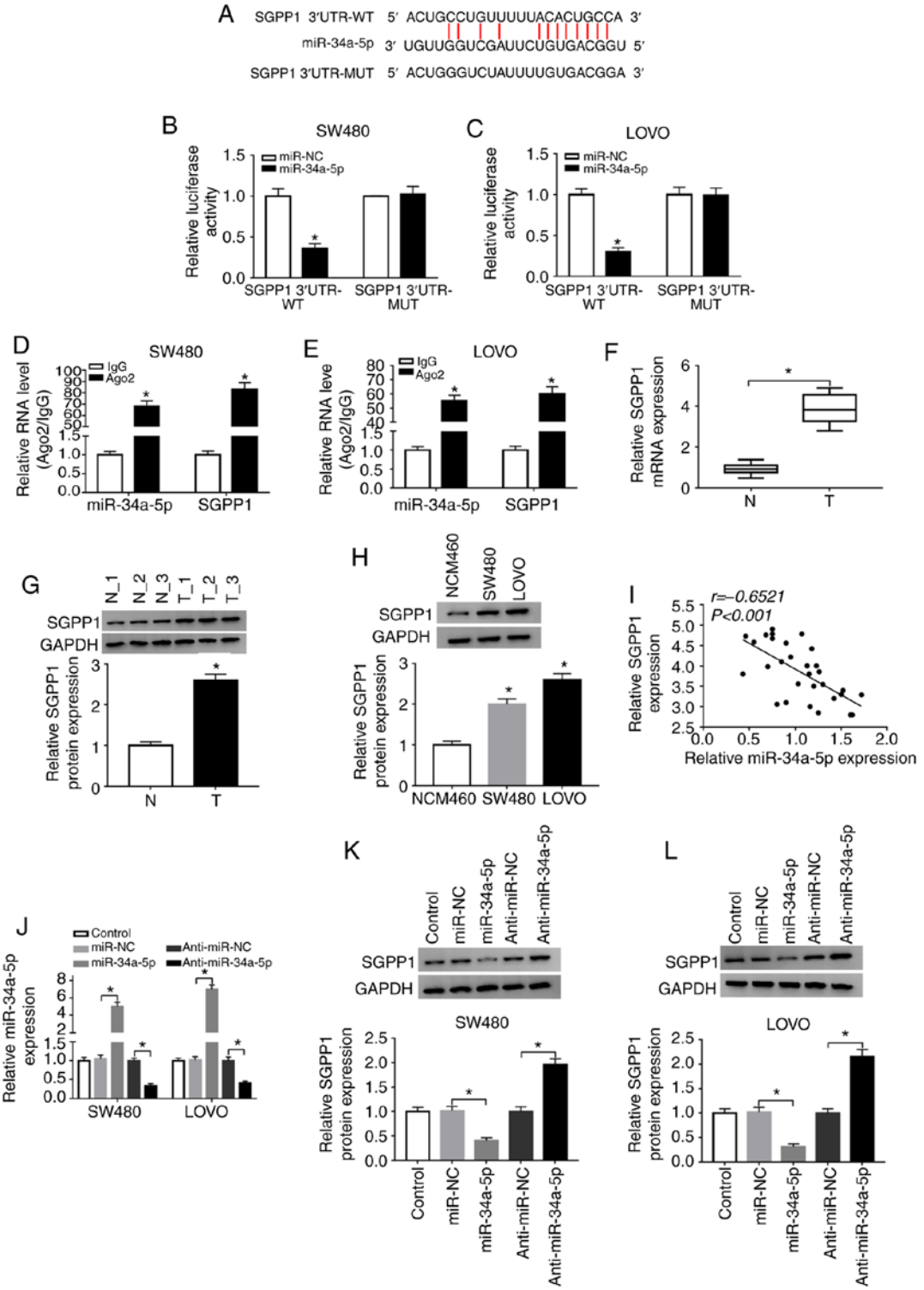

Figure 6. miR-34a-5p directly interacts with SGPP1 and negatively regulates SGPP1 expression. (A) The predicted binding sites between miR-34a-5p and SGPP1. (B and C) The luciferase activity in miR-NC or miR-34a-5p and SGPP1 3'UTR-WT or SGPP1 3'UTR-MUT co-transfected SW480 and LOVO cells was measured by dual-luciferase reporter assay. *P<0.05 vs. the miR-NC group. (D and E) The levels of miR-34a-5p and SGPP1 in Ago2 or IgG immunoprecipitation complexes in SW480 and LOVO cells were detected by RT-qPCR assay. *P<0.05 vs. the IgG group. (F and G) RT-qPCR assay and western blotting were conducted to examine the mRNA and protein levels of SGPP1 in the serums collected from colon cancer patients and healthy participants, respectively. *P<0.05 vs. the normal group. (H) The protein level of SGPP1 in NCM460, SW480 and LOVO cells was examined by western blotting. *P<0.05 vs. the NCM460 group. (I) The correlation between SGPP1 and miR-34a-5p was analyzed by Spearman's correlation coefficient analysis. (J-L) The expression of miR-34a-5p and SGPP1 in SW480 and LOVO cells transfected with miR-NC, miR-34a-5p, anti-miR-NC or anti-miR-34a-5p was detected by RT-qPCR and western blotting, respectively. *P<0.05 vs. miR-NC or the anti-miR-NC group. miR, microRNA; SGPP1, sphingosine-1-phosphate phosphatase 1; NC, negative control; WT, wild-type; MUT, mutated; Ago2, Argonaute2; IgG, immunoglobulin G; RT-qPCR, reverse transcription-quantitative polymerase chain reaction.

circ-HMGCS1. Gao *et al* revealed that miR-34a-5p was downregulated in CRC, and ectopic expression of miR-34a-5p suppressed cell growth and metastasis and induced apoptosis in CRC (21). Sun *et al* demonstrated that miR-34a inhibitors

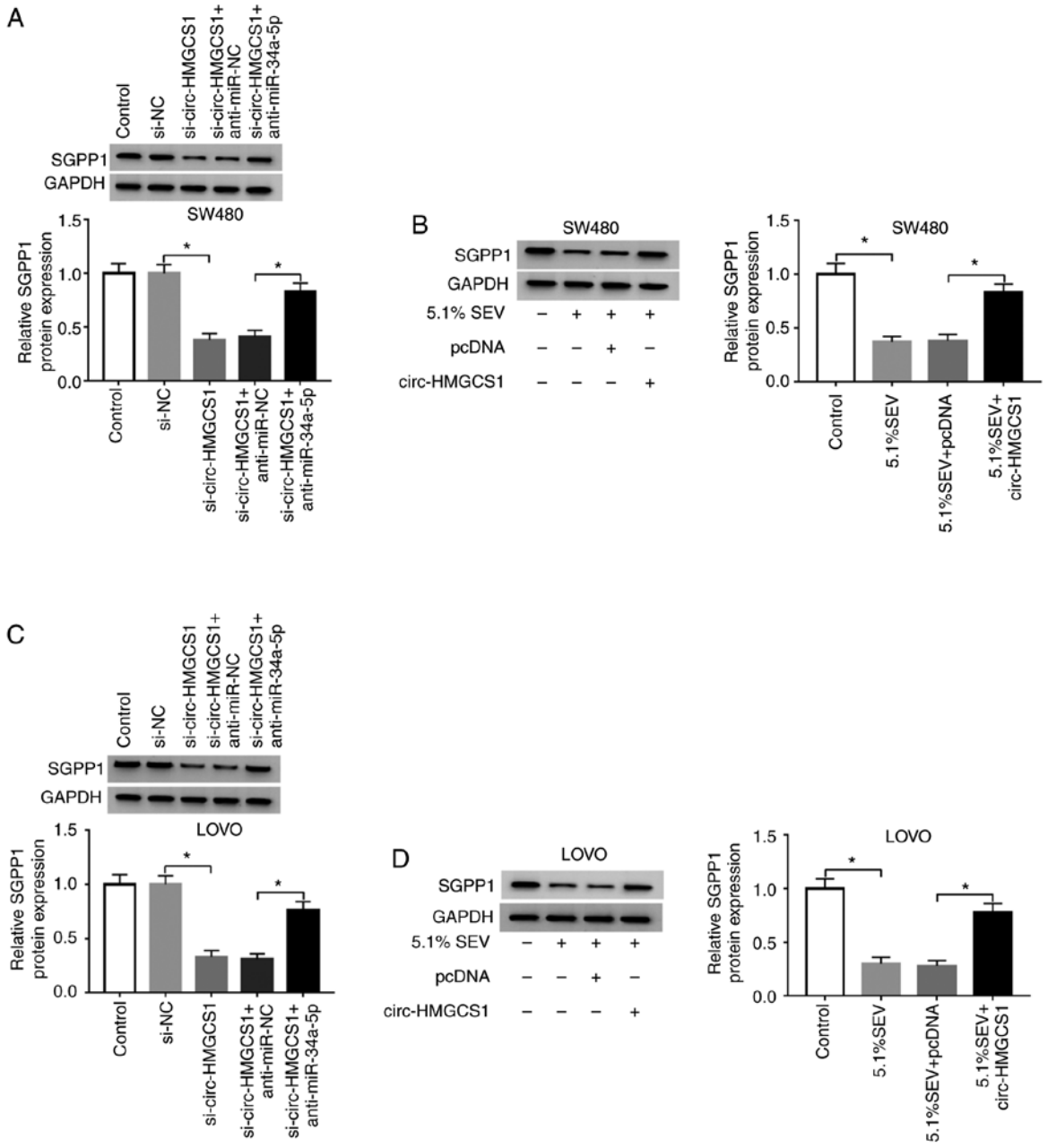

Figure 7. Sevoflurane decreases SGPP1 expression by regulating the circ-HMGCS1/miR-34a-5p axis in colon cancer cells. (A and C) SW480 and LOVO cells were assigned to Control, si-NC, si-circ-HMGCS1, si-circ-HMGCS1+anti-miR-NC and si-circ-HMGCS1+anti-miR-34a-5p groups. *P<0.05 vs. si-NC or si-circ-HMGCS1+anti-miR-NC. (B and D) SW480 and LOVO cells were assigned to Control, 5.1% SEV, 5.1% SEV+pcDNA and 5.1% SEV+circ-HMGCS1 groups. *P<0.05 vs. the control group or the 5.1% SEV+pcDNA group. (A-D) SGPP1 protein levels in SW480 and LOVO cells was analyzed using western blotting. circ-HMGCS1, circular RNA 3-hydroxy-3-methylglutaryl-CoA synthase 1; miR, microRNA; si, small interfering; NC, negative control; SEV, sevoflurane; SGPP1, sphingosine-1-phosphate phosphatase 1.

restored the inhibitory effects of sevoflurane on CRC cell viability and metastasis by binding to ADAM10 (31). In line with these data, we revealed that the suppressive roles of circ-HMGCS1 silencing on cell viability and invasion and the promoting role of circ-HMGCS1 silencing in cell apoptosis in colon cancer were all reversed by miR-34a-5p inhibition. Moreover, miR-34a-5p inhibition could reverse the inhibition in the progression of colon cancer cells caused by sevoflurane treatment. In addition, it was revealed that SGPP1 was a direct target gene of miR-34a-5p. Gao *et al* demonstrated that SGPP1 was increased in CRC tissues and cells, and miR-27a could target SGPP1 to hinder cell growth and migration and facilitate cell apoptosis in CRC (21). In the present study, SGPP1 was increased in colon cancer patients and cells and SGPP1 was negatively modulated by miR-34a-5p. Moreover, it was revealed that circ-HMGCS1 could promote SGPP1 expression through sponging miR-34a-5p.

In summary, sevoflurane hindered cell viability and invasion and facilitated cell apoptosis in colon cancer by regulating the exosome-transmitted circ-HMGCS1/miR-34a-5p/SGPP1 axis. These findings facilitated our understanding of sevoflurane on colon cancer progression and may provide an experimental basis for selecting more reasonable anesthetics for patients.

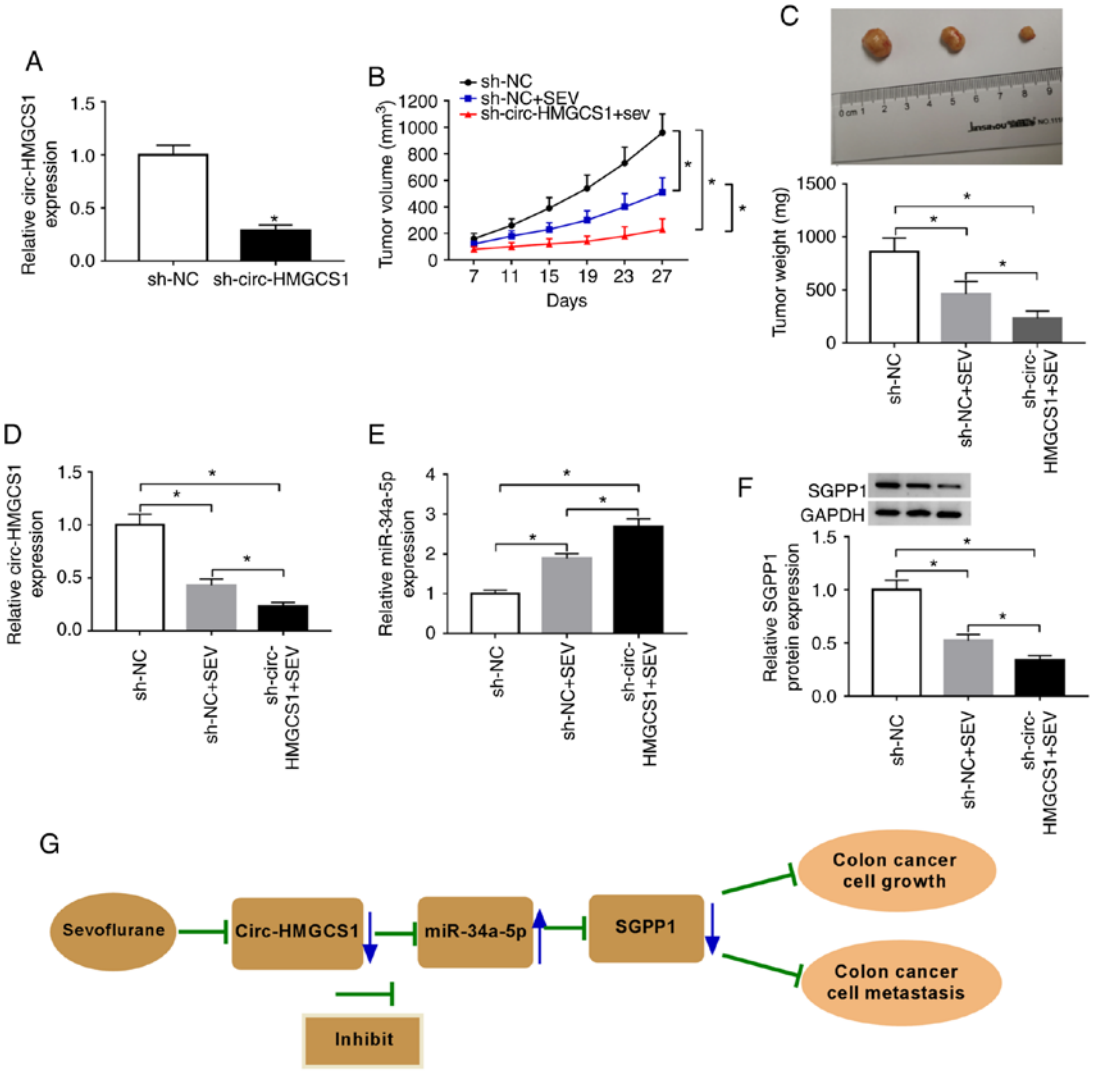

Figure 8. Circ-HMGCS1 silencing suppresses tumor growth of colon cancer *in vivo*. The mice were divided into 2 groups: sh-NC+SEV and sh-circ-HMGCS1+SEV. (A) The expression level of circ-HMGCS1 in SW480 cells transfected with sh-circ-HMGCS1 or sh-NC was determined by RT-qPCR assay. (B) The tumor volume was measured every 4 days from the 7th day. (C) The tumor weight was examined after cells were injected for 27 days. (D and E) The levels of circ-HMGCS1 and miR-34a-5p in the collected tumors were determined by RT-qPCR. (F) The level of SGPP1 in the collected tumors was detected by western blotting. (G) The working model of sevoflurane in colon cancer progression is presented. *P<0.05 vs. sh-NC group or as indicated in the images. circ-HMGCS1, circular RNA 3-hydroxy-3-methylglutaryl-CoA synthase 1; sh, short hairpin; NC, negative control; SEV, sevoflurane; miR, microRNA; RT-qPCR, reverse transcription-quantitative polymerase chain reaction.

Acknowledgements

Not applicable.

Funding

No funding was received.

Availability of data and materials

The analyzed data sets generated during the present study are available from the corresponding author on reasonable request.

Authors' contributions

Conceptualization and methodology was performed by JH, HZ and XL. DW, YW and YA performed the formal analysis and data curation. JH and JY conducted the validation and investigation. JH, HZ, XL and DW drafted the manuscript, wrote, reviewed and edited the manuscript. All authors approved the final manuscript and agreed be accountable for all aspects of the work in ensuring that questions related to the accuracy or integrity of any part of the work are appropriately investigated and resolved.

Ethics approval and consent to participate

The present study was approved by the Ethics Review Committee of The First Affiliated Hospital of Zhengzhou University. Written informed consent was obtained from all enrolled patients. The animal experiments were approved by the Ethics Committee of Animal Research of the First Affiliated Hospital of Zhengzhou University.

Patient consent for publication

Not applicable.

Competing interests

The authors declare that they have no competing interests.

References

1. Siegel RL, Miller KD, Fedewa SA, Ahnen DJ, Meester RGS, Barzi A and Jemal A: Colorectal cancer statistics, 2017. CA Cancer J Clin 67: 177-193, 2017.
2. Siegel RL, Miller KD and Jemal A: Cancer statistics, 2016. CA Cancer J Clin 66: 7-30, 2016.
3. Bray F, Ferlay J, Soerjomataram I, Siegel RL, Torre LA and Jemal A: Global cancer statistics 2018: GLOBOCAN estimates of incidence and mortality worldwide for 36 cancers in 185 countries. CA Cancer J Clin 68: 394-424, 2018.
4. Moriarity A, O'Sullivan J, Kennedy J, Mehigan B and McCormick P: Current targeted therapies in the treatment of advanced colorectal cancer: A review. Ther Adv Med Oncol 8: 276-293, 2016.
5. Vasile L, Olaru A, Munteanu M, Plesea IE, Surlin V and Tudorascu C: Prognosis of colorectal cancer: Clinical, pathological and therapeutic correlation. Rom J Morphol Embryol 53: 383-391, 2012.
6. Green JS and Tsui BC: Impact of anesthesia for cancer surgery: Continuing professional development. Can J Anaesth 60: 1248-1269, 2013.
7. Liang H, Gu M, Yang C, Wang H, Wen X and Zhou Q: Sevoflurane inhibits invasion and migration of lung cancer cells by inactivating the p38 MAPK signaling pathway. J Anesth 26: 381-392, 2012.
8. Gao C, Shen J, Meng ZX and He XF: Sevoflurane Inhibits Glioma Cells Proliferation and Metastasis through miRNA-124-3p/ROCK1 Axis. Pathol Oncol Res 26: 947-954, 2020.
9. Sun Z, Shi K, Yang S, Liu J, Zhou Q, Wang G, Song J, Li Z, Zhang Z and Yuan W: Effect of exosomal miRNA on cancer biology and clinical applications. Mol Cancer 17: 147, 2018.
10. Sundararajan V, Sarkar FH and Ramasamy TS: The multifaceted role of exosomes in cancer progression: Diagnostic and therapeutic implications [corrected]. Cell Oncol (Dordr) 41: 223-252, 2018.
11. Nedaeinia R, Manian M, Jazayeri MH, Ranjbar M, Salehi R, Sharifi M, Mohaghegh F, Goli M, Jahednia SH, Avan A and Ghayour-Mobarhan M: Circulating exosomes and exosomal microRNAs as biomarkers in gastrointestinal cancer. Cancer Gene Ther 24: 48-56, 2017.
12. Li X, Yang L and Chen LL: The biogenesis, functions, and challenges of circular RNAs. Mol Cell 71: 428-442, 2018.
13. Zhang Q, Zhang C, Ma JX, Ren H, Sun Y and Xu JZ: Circular RNA PIP5K1A promotes colon cancer development through inhibiting miR-1273a. World J Gastroenterol 25: 5300-5309, 2019.
14. Xu XW, Zheng BA, Hu ZM, Qian ZY, Huang CJ, Liu XQ and Wu WD: Circular RNA hsa_circ_000984 promotes colon cancer growth and metastasis by sponging miR-106b. Oncotarget 8: 91674-91683, 2017.
15. Zhen N, Gu S, Ma J, Zhu J, Yin M, Xu M, Wang J, Huang N, Cui Z, Bian Z, *et al*: CircHMGCS1 promotes hepatoblastoma cell proliferation by regulating the IGF signaling pathway and glutaminolysis. Theranostics 9: 900-919, 2019.
16. Dong J, Li J, Luo J and Wu W: CircHMGCS1 is upregulated in colorectal cancer and promotes proliferation of colorectal cancer cells by targeting microRNA-503-5p. Eur J Inflam:17: 1-11, 2019.
17. Reddy KB: MicroRNA (miRNA) in cancer. Cancer Cell Int 15: 38, 2015.
18. Luan XF, Wang L and Gai XF: The miR-28-5p-CAMTA2 axis regulates colon cancer progression via Wnt/beta-catenin signaling. J Cell Biochem: Nov 10, 2019 (Epub ahead of print). doi: 10.1002/jcb.29536.
19. Chai B, Guo Y, Cui X, Liu J, Suo Y, Dou Z and Li N: MiR-223-3p promotes the proliferation, invasion and migration of colon cancer cells by negative regulating PRDM1. Am J Transl Res 11: 4516-4523, 2019.
20. Xi X, Teng M, Zhang L, Xia L, Chen J and Cui Z: MicroRNA-204-3p represses colon cancer cells proliferation, migration, and invasion by targeting HMGA2. J Cell Physiol 235: 1330-1338, 2019.
21. Gao J, Li N, Dong Y, Li S, Xu L, Li X, Li Y, Li Z, Ng SS, Sung JJ, *et al*: miR-34a-5p suppresses colorectal cancer metastasis and predicts recurrence in patients with stage II/III colorectal cancer. Oncogene 34: 4142-4152, 2015.
22. Kara M, Yumrutas O, Ozcan O, Celik OI, Bozgeyik E, Bozgeyik I and Tasdemir S: Differential expressions of cancer-associated genes and their regulatory miRNAs in colorectal carcinoma. Gene 567: 81-86, 2015.
23. Bao Y, Chen Z, Guo Y, Feng Y, Li Z, Han W, Wang J, Zhao W, Jiao Y, Li K, *et al*: Tumor suppressor microRNA-27a in colorectal carcinogenesis and progression by targeting SGPP1 and Smad2. PLoS One 9: e105991, 2014.
24. Lässer C, Eldh M and Lötvall J: Isolation and characterization of RNA-containing exosomes. J Vis Exp: e3037, 2012.
25. Livak KJ and Schmittgen TD: Analysis of relative gene expression data using real-time quantitative PCR and the 2(-Delta Delta C(T)) method. Methods 25: 402-408, 2001.
26. Niwa H, Rowbotham DJ, Lambert DG and Buggy DJ: Can anesthetic techniques or drugs affect cancer recurrence in patients undergoing cancer surgery? J Anesth 27: 731-741, 2013.
27. Yang X, Zheng YT and Rong W: Sevoflurane induces apoptosis and inhibits the growth and motility of colon cancer in vitro and in vivo via inactivating Ras/Raf/MEK/ERK signaling. Life Sci 239: 116916, 2019.
28. Fan L, Wu Y, Wang J, He J and Han X: Sevoflurane inhibits the migration and invasion of colorectal cancer cells through regulating ERK/MMP-9 pathway by up-regulating miR-203. Eur J Pharmacol 850: 43-52, 2019.
29. Militello G, Weirick T, John D, Doring C, Dimmeler S and Uchida S: Screening and validation of lncRNAs and circRNAs as miRNA sponges. Brief Bioinform 18: 780-788, 2017.
30. Rong D, Sun H, Li Z, Liu S, Dong C, Fu K, Tang W and Cao H: An emerging function of circRNA-miRNAs-mRNA axis in human diseases. Oncotarget 8: 73271-73281, 2017.
31. Sun SQ, Ren LJ, Liu J, Wang P and Shan SM: Sevoflurane inhibits migration and invasion of colorectal cancer cells by regulating microRNA-34a/ADAM10 axis. Neoplasma 66: 887-895, 2019.